matrix. The polymer branches may be distributed both on the surface of the internal macropore and in the amorphous domain of the polymer matrix. The distribution ratio causes the difference in the water permeability of the monomer-grafted membrane. For simultaneous irradiation grafting, a higher amount of the polymer branches is grafted in the polymer matrix because the radical reacts with monomer previously penetrated in the polymer matrix before irradiation. In contrast, for preirradiation grafting, the monomer needs to be diffused into the polymer matrix toward the radical after irradiation, and thus a higher amount of the polymer branches is grafted on the surface of the internal macropore. When the irradiated membrane is exposed to air before grafting, the radical on the surface of the internal macropore decays instantaneously because of the oxygen diffusion. Therefore, the monomer will invade the polymer matrix more deeply compared to the preirradiation grafting without exposure to air. A higher amount of the polymer branches in the polymer matrix than on the surface of the internal macropore results in a higher swelling ratio and PWF of the monomer-grafted membrane.

In summary, we have found that we can control the location of the polymer branches grafted onto the porous material by selecting not only the combination of trunk polymer and monomer but also the grafting technique, such as simultaneous/preirradiation grafting with/without exposure to air. This principle may be of interest for modifying existing porous materials into the functional porous materials by radiation-induced graft polymerization.

Photochemical Preparation of Crystalline Silicon Nanoclusters

J. M. Jasinski* and F. K. LeGoues

IBM Research Division
Thomas J. Watson Research Center
Yorktown Heights, New York 10598

Received July 11, 1991
Revised Manuscript Received August 29, 1991

There is considerable current interest in the preparation and properties of nanometer-size semiconductor crystallites.[1] Such nanoclusters exhibit novel materials properties largely as a consequence of their finite small size. Most of the existing work on semiconductor nanoclusters has concentrated on II-VI, IV-VI, and III-V materials such as CdS, PbS, and GaAs. There have been very few reports of the preparation of group IV nanoclusters. Some results are available for Ge nanoclusters prepared by gas evaporation methods[2] and for Ge nanoclusters isolated in SiO_2 which are prepared by cosputtering.[3] In addition, quantum size effects have been attributed to microcrystalline silicon films and silicon nanoparticles prepared by slow discharge methods.[4] Intriguing results, such as tunable visible photoluminescence, have also been reported for electrochemically etched samples of silicon, with the effects being attributed to the formation of quantum wires in the material.[5]

A difficulty in the preparation of discrete group IV nanoclusters, compared to the preparation of compound semiconductor materials, is an apparent lack of synthetic chemical methods for their preparation. In this paper we report the unexpected finding that silicon nanoclusters can be formed in the gas-phase, room-temperature photolysis of disilane with the output from an ArF excimer laser operating at 193 nm. This observation may lead ultimately to the preparation of useful macroscopic quantities of these materials for further study and possible applications in silicon-based optoelectronics and nonlinear optics.

Photolysis of disilane has been used by various groups over the past 10 years to deposit silicon films ranging in crystallinity from amorphous hydrogenated silicon to epitaxial silicon.[6] Several studies of the photochemistry of disilane at 193 nm have also been carried out.[7-10] The photodissociation process is exceedingly complicated, with numerous possible product channels and the generation of numerous possible silicon hydride reactive intermediates. There have also been reports of the formation of hydrogenated amorphous silicon powder under various photolysis conditions.[11,12] This process is normally viewed as detrimental to thin-film deposition. By exercising some control over the photolysis conditions, we find that we can turn the "nuisance" of gas-phase powder formation into a potentially useful synthetic pathway for the formation of silicon nanoclusters.

Samples were prepared by the photolysis of disilane dilute in helium buffer gas in a stainless steel flow cell which is identical in all important aspects to those we have previously described in studies of the spectroscopy and kinetics of silicon hydride reactive intermediates.[13] The cell was evacuated with an mechanical pump and was operated under conditions of constant total flow and constant total pressure. The base pressure of the system was in the milliTorr range. The total flow was 100 sccm and the total pressure was 5 Torr in all experiments. The disilane partial pressure was varied from 0 to 200 mTorr. From the measured leak/outgassing rate of the cell, we estimate that the partial pressure of oxygen, water, and hydrocarbons was in the 10^{-4}-Torr range during depositions. The higher quality samples (smallest crystallites) were typically deposited with a disilane partial pressure of 15–25 mTorr. The photolysis source was the unfocused output of an ArF excimer laser operating at 193 nm. The laser beam entered the cell through a helium-purged Su-

---

(1) Bawendi, M.; Steigerwald, M. L.; Brus, L. E. *Annu. Rev. Phys. Chem.* **1990**, *41*, 477. Wang, Y.; Herron, N. *J. Phys. Chem.* **1991**, *95*, 525.

(2) Hayashi, S.; Wakayama, H.; Okada, T.; Kim, S. S.; Yamamoto, K. *J. Phys. Soc. Jpn.* **1987**, *56*, 243.

(3) Fujii, M.; Hayashi, S.; Yamamoto, K. *Jpn. J. Appl. Phys.* **1991**, *30*, 687. Hayashi, S.; Fujii, M.; Yamamoto, K. *Jpn. J. Appl. Phys. Lett.* **1989**, *28*, L1464. Fujii, M.; Hayashi, S.; Yamamoto, K. *Appl. Phys. Lett.* **1990**, *57*, 2692.

(4) Furukawa, S.; Miyasato, T. *Phys. Rev. B* **1988**, *38*, 5726. Takagi, H.; Ogawa, H.; Yamazaki, Y.; Ishizaki, A.; Nakagiri, T. *Appl. Phys. Lett.* **1990**, *56*, 2379.

(5) Canham, L. T. *Appl. Phys. Lett.* **1990**, *57*, 1046.

(6) See, for example: Mishima, Y.; Hirose, M.; Osaka, Y.; Nagamine, K.; Ashida, Y.; Kitagawa, N.; Isogaya, K. *Jpn. J. Appl. Phys. Lett.* **1983**, *22*, L46. Yoshikawa, A.; Yamaga, S. *Jpn. J. Appl. Phys. Lett.* **1984**, *23*, L91. Lian, S.; Fowler, B.; Bullock, D.; Banerjee, S. *Appl. Phys. Lett.* **1991**, *58*, 514.

(7) Stafast, H. *Appl. Phys. A* **1988**, *45*, 93.

(8) Chu, J. O.; Begemann, M. H.; McKillop, J. S.; Jasinski, J. M. *Chem. Phys. Lett.* **1989**, *155*, 576. Jasinski, J. M. *Chem. Phys. Lett.*, **1991**, *183*, 558.

(9) Eres, D.; Geohegan, D. B.; Lowndes, D. H.; Mashburn, D. N. *Appl. Surf. Sci.* **1989**, *36*, 70.

(10) Muranaka, Y.; Motooka, T.; Lubben, D.; Greene, J. E. *J. Appl. Phys.* **1989**, *66*, 910.

(11) Jasinski, J. M.; Chu, J. O.; Begemann, M. H. *Mater. Res. Soc. Symp. Proc.* **1989**, *131*, 487.

(12) Dietrich, T. R.; Chiussi, S.; Stafast, H.; Comes, F. J. *Appl. Phys. A* **1989**, *48*, 405.

(13) Jasinski, J. M. *J. Phys. Chem.* **1986**, *90*, 555. Jasinski, J. M.; Chu, J. O. *J. Chem. Phys.* **1988**, *88*, 1678.

0897-4756/91/2803-0989$02.50/0

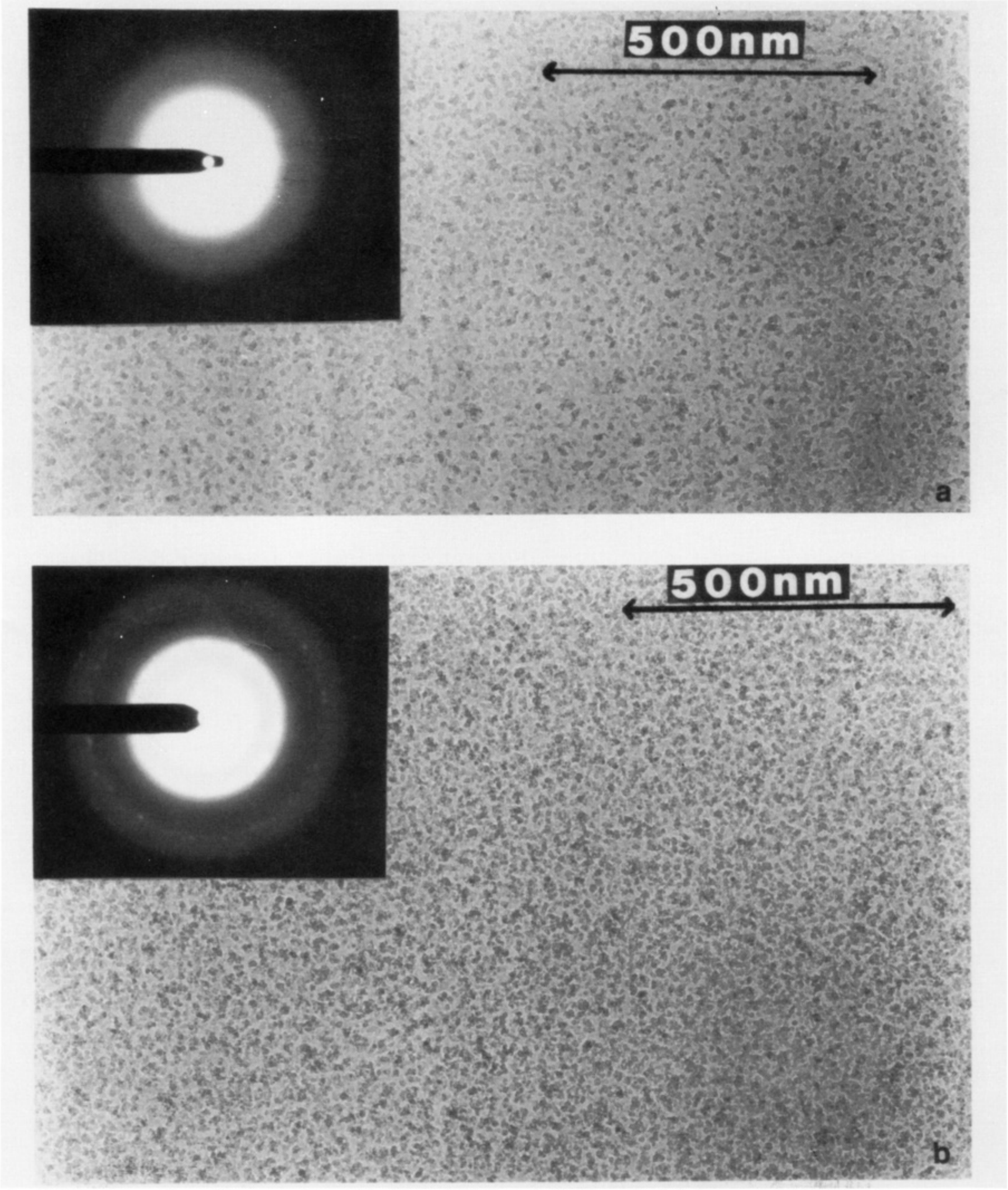

Figure 1. TEM images of samples grown from 15 mTorr of disilane in helium at a total pressure of 5 Torr. Laser repetition rate was (a) 0.7 and (b) 4 Hz. The sample in a shows an amorphous electron diffraction pattern. The sample in b shows a crystalline diffraction pattern superimposed on an amorphous background.

prasil window. The output fluence of the laser was typically 90 mJ cm^{-2} pulse^{-1}, and approximately half of that fluence actually entered the photolysis cell. The excimer laser repetition rate was typically 4 Hz but was varied from 0.7 to 12.8 Hz (vide infra). Samples for transmission electron microscopy (TEM) were deposited directly onto amorphous carbon substrates (Ladd Research, supported on 300-mesh Cu grids), which were suspended in the photolysis cell using a Gatan ion mill sample holder. Bulk samples were deposited onto Pyrex or NaCl substrates. The laser beam was parallel to and grazing the substrate surface in all cases. Deposition time for TEM samples was 20–60 min, depending on the disilane partial pressure and the excimer laser repetition rate. Bulk samples were deposited at 15 mTorr disilane partial pressure at an excimer laser repetition rate of 4 Hz. Deposition times were 2.5–4 h.

TEM samples were examined in a Philips 430 microscope operating at 300 kV. Energy-dispersive X-ray analysis (EDX) was used in the TEM in order to ascertain that the observed clusters contained silicon. Bulk samples were characterized by UV–vis absorption spectroscopy, FTIR spectroscopy, and X-ray diffraction using commercially available spectrometers.

Figure 1 shows TEM results for two samples. Both samples were prepared using a disilane partial pressure of 15 mTorr. The insets in Figure 1 show electron diffraction patterns, which demonstrate that the sample in Figure 1a is amorphous, while that in Figure 1b shows crystallinity. Since the clusters were deposited onto an amorphous

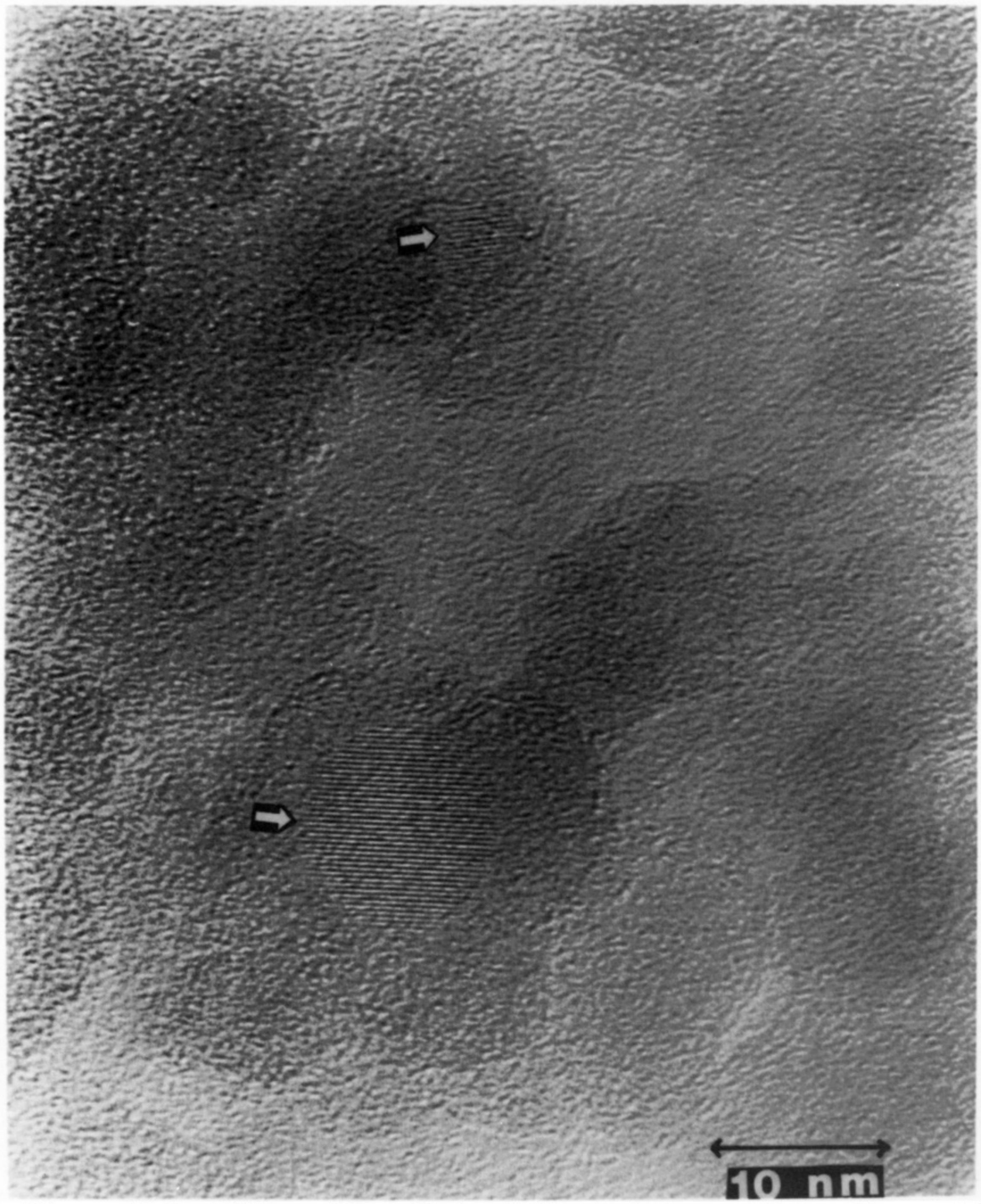

Figure 2. Higher magnification TEM image of the sample shown in Figure 1b showing several clusters. The arrows indicate two clusters oriented with the [111] crystal planes parallel to the electron beam so that lattice images of the [111] planes are visible. The smaller cluster is about 4 nm in size, and the larger cluster is about 11 nm in size.

carbon film, the diffraction patterns, for both samples, will show a strong amorphous background (the typical "amorphous rings" clearly seen in Figure 1a). It is thus impossible to tell from Figure 1b whether all the clusters are crystalline or whether we have a mixture of amorphous and crystalline clusters. The diffraction pattern shown in Figure 1b is that expected for randomly oriented crystallites with a lattice parameter of unstrained silicon. The amorphous sample was prepared using an excimer laser repetition rate of 0.7 Hz. The crystalline sample was prepared using an excimer laser repetition rate of 4 Hz. The slower repetition rate corresponds to a time between laser pulses which is *longer* than the average residence time of gas and clusters in the photolysis cell. The higher repetition rate corresponds to several laser pulses entering the cell during the average residence time.

Figure 2 shows a high-resolution micrograph where two clusters (see arrows) have their [111] planes parallel to the electron beam, so that lattice images can be obtained. This indicates that individual clusters which are crystalline have a single orientation. An amorphous SiO_2 layer may be present at the surface of each crystalline cluster, since the samples have been transported in air, but it is very difficult to image such a layer against a background of amorphous carbon. The smallest crystallites for which lattice images were observed were in the 3 nm range.

From a series of TEM samples prepared under different conditions, the following general observations were made: (1) Crystalline clusters are observed only when the time between laser pulses is shorter than the average residence time of gas in the cell. (2) The size of the clusters correlates with disilane partial pressure, higher partial pressures resulting in larger clusters and vice versa. (3) The average size of the particles does not change noticeably as a function of laser repetition rate, over the range 0.7–12.8 Hz. (4) No clusters are observed on the grids if the photolysis is carried out in the absence of disilane. (5) The crystalline clusters were typically in the 3–10-nm size range. No further characterization of the size distribution was possible since the larger area microscope images did not have suitable contrast to be digitized and analyzed. Observation 1 suggests that the clusters initially grow as amorphous material in the gas phase following a single laser pulse and are annealed and crystallized in the gas phase by subsequent laser pulses. Observation 2 is consistent with the growth being from gas-phase intermediates and/or adsorption of disilane onto the surface of nucleated clusters. Observation 3 supports the contention that the clusters grow as the result of a single laser pulse. If growth were the result of repeated pulses, then higher laser repetition rates should lead to larger and larger clusters. This is not observed. Observation 4 serves as a control and rules out laser sputtering of material from cell windows, walls, or the substrate holder as the source of clusters. The detailed growth mechanism of the clusters remains to be studied, and it is possible that the process is more complicated than that suggested above. It is important to note, however, that the disilane partial pressure has the most pronounced effect on cluster size and the laser repetition rate, relative to the average residence time of clusters in the cell, has the most pronounced effect on cluster morphology. The TEM samples were routinely handled and transported in air. They were stored in a nitrogen-purged desiccator for periods of weeks and were shown to remain crystalline by electron diffraction.

Several bulk samples were also prepared. Qualitatively, these samples have an optical gap similar to that of microcrystalline silicon and an infrared spectrum which resembles that of a heavily hydrogenated phase.[14] The samples were transparent adherent films with a yellowish color. The UV–vis spectrum of one such sample was obtained by scraping the material off a glass substrate and suspending the sample in ethanol. From this spectrum, an optical gap of 1.8 eV was determined from a plot of $(\alpha E)^{1/2}$ vs E, where α is the optical density and E is the photon energy (Tauc plot).[5,15] The infrared spectrum of the samples, obtained on a NaCl substrate, indicates that hydrogen is present. The strongest bands occur at 2100, 1250, 910, and 870 cm^{-1}. With the exception of the band at 1250 cm^{-1}, the remaining bands correspond reasonably well to those assigned to SiH_2 and/or SiH_3 groups in the hydrogenated silicon literature. It is possible that the 1250 cm^{-1} is the first overtone of a strong SiH_x mode which is normally seen at 630 cm^{-1} and is just at the cutoff of the NaCl substrate. No X-ray diffraction pattern above background could be observed from any of the bulk samples. One such sample was scraped from the substrate following the diffraction scan, taken up in ethanol, dropped onto a TEM grid and examined. The sample showed a strongly crystalline electron diffraction pattern and the presence of nanocrystals. The bulk samples oxidized slowly over the course of a few days in air as evidenced by the appearance of a strong SiO stretching band at $\simeq$1080 cm^{-1} in the FTIR spectrum.[14,15] While the TEM results provide unequivocal evidence that crystalline nanoclusters are produced, the results for the bulk samples suggest that a substantial amount of heavily hydrogenated amorphous material may also be present.

In conclusion, we have demonstrated that crystalline silicon nanoclusters are formed in the gas-phase laser photolysis of disilane dilute in helium at room temperature. The experiments strongly suggest that the clusters grow as amorphous material which is annealed and crystallized in the gas phase by subsequent laser pulses. This represents a rational photochemical synthesis of silicon nanoclusters. Further work is clearly required to determine the factors which most strongly control the average cluster size and the size distribution, as well as to accurately characterize the bulk samples. Finally, we note that the photochemical method described above should be compatible with the preparation of n-type and p-type doped nanoclusters by cophotolysis of phosphine, arsine, or diborane,[16] the preparation of germanium nanoclusters by photolysis of digermane,[17] and the preparation of silicon–germanium alloys by cophotolysis of disilane and digermane.

Acknowledgment. We thank Ivan Haller for assistance with the UV–visible spectra, Bruce Scott, Joe Bringley, and Armin Segmuller for X-ray diffraction studies, and Paul Alivisatos for a stimulating discussion.

Registry No. Silicon, 7440-21-3; disilane, 1590-87-0.

---

[14] *Properties of Amorphous Silicon*; EMIS Datareviews Series No. 1; Institute of Electrical Engineers: Surrey, England, 1985.

[15] Richter, H.; Ley, L. *J. Appl. Phys.* **1981**, *52*, 7281.

[16] Clark, J. H.; Anderson, R. G. *Appl. Phys. Lett.* **1978**, *32*, 46.

[17] Eres, D.; Lowndes, D. H.; Tischler, J. Z.; Sharp, J. W.; Geohegan, D. B.; Pennycook, S. J. *Mater. Res. Soc. Symp. Proc.* **1989**, *131*, 517.

Intercalation of Poly(ethylene oxide) in V_2O_5 Xerogel

Y.-J. Liu,[†] D. C. DeGroot,[‡] J. L. Schindler,[‡] C. R. Kannewurf,[‡] and M. G. Kanatzidis*,[†]

Department of Chemistry and
Center of Fundamental Materials Research
Michigan State University
East Lansing, Michigan 48824
Department of Electrical Engineering and
Computer Science
Northwestern University, Evanston, Illinois 60208

Received July 11, 1991
Revised Manuscript Received September 9, 1991

$V_2O_5 \cdot nH_2O$ is a porous solid with a layered structure, and it is capable of diverse intercalation chemistry.[1] This material can be easily fabricated into films and coatings and can act as a host lattice by accepting neutral or charged guest species.[2-4] Intercalation can involve cation

---

[†] Michigan State University.

[‡] Northwestern University.

[1] (a) Lemerle, J.; Nejem, L.; Lefebvre, J. *J. Inorg. Nucl. Chem.* **1980**, *42*, 17–20. (b) Bullot, J.; Gallais, O.; Gauthier, M.; Livage, J. *Appl. Phys. Lett.* **1980**, *36*, 986–988. (c) Sanchez, C.; Babonneau, F.; Morineau, R.; Livage, J.; Bullot, J. *Philos. Mag., Part B* **1983**, *47*, 279–290.

[2] (a) Legendre, J.-J.; Livage, J. *J. Colloid Interface Sci.* **1983**, *94*, 75–83. (b) Legendre, J. J.; Aldebert, P.; Baffier, N.; Livage, J. *J. Colloid Interface Sci.* **1983**, *94*, 84–89. (c) Aldebert, P.; Haesslin, H. W.; Baffier, N.; Livage, J. *J. Colloid Interface Sci.* **1983**, *98*, 478–483. (d) Gharbi, N.; Sanchez, C.; Livage, J.; Lemerle, J.; Nejem, L.; Lefebvre, J. *Inorg. Chem.* **1982**, *21*, 2758–2765.

[3] (a) Aldebert, P.; Baffier, N.; Legendre, J.-J.; Livage, J. *Rev. Chim. Miner.* **1982**, *19*, 485–495. (b) Lemordant, D.; Bouhaouss, A.; Aldebert, P.; Baffier, N. *J. Chim. Phys.* **1986**, *83*, 105–113. (c) Aldebert, P.; Baffier, N.; Gharbi, N.; Livage, J. *Mater. Res. Bull.* **1981**, *16*, 949–955.

[4] Livage, J. *J. Solid State Chem.* **1986**, *64*, 322–330.

0897-4756/91/2803-0992$02.50/0